

# DC SEPTUM MAGNET WITH LOW CURRENT DENSITY FOR THE SYNCHROTRON LIGHT SOURCE\*

H. Yamaguchi<sup>†</sup>, T. Taniuchi, K. Fukami<sup>1</sup>, T. Aoki, S. Takano<sup>1</sup>, T. Watanabe<sup>1</sup>

Japan Synchrotron Radiation Research Institute, Hyogo, Japan

Y. Takemura, SPring-8 Service Co., Ltd., Tatsuno, Japan

<sup>1</sup> also at RIKEN SPring-8 Center (RSC), Hyogo, Japan

## Abstract

We newly designed and fabricated a new DC septum magnet. Conventional direct-drive DC septa are embedded with coils inside the magnet gap, which usually results in rather high current density in the thinner septum conductor. It can, however, lead to failures in coils due to harsh heat cycles and faults in high-current power supplies. We propose an alternative septum magnet design to reduce the coil current density by an order of magnitude that achieves a high flux density of 1.2 T with the current density with the 5 mm thick septum. We present our new magnet design and the measured performance of the magnet.

## INTRODUCTION

Magnets near the beam injection point on the beam transport line are designed to deflect the injected beam while avoiding interference with the stored beam in the storage ring. Therefore, such magnets generally have magnetic shields between the injected and the stored beam. The shield is called “septum”. In a conventional direct-drive type DC septum magnet, the coil is implemented in a magnet pole gap. The current density in the coil tends to be higher due to the small cross-section of the coil attributed to the short distance between the injected and the stored beam. Such higher coil current density imposes huge work and costs in the design, production, and maintenance of both the magnet and the power supply. Moreover, the high coil current density induces large electric power consumption. For example, DC septum magnets at SPring-8, which is a direct-drive type, the coil current density and power consumption are approximately 70 A/mm<sup>2</sup> and 40 kW, respectively [1]. That is the most power consuming magnet in the facility. In this paper, we present a DC septum magnet with low coil current density designed by optimizing the profile of the septum shield to apply not only to SPring-8 but also to future light source facilities.

## DESIGN

Our DC septum magnet is designed as a rectangular magnet for manufacture and alignment to be simple. The magnetic field in the magnet poles and the effective magnetic length are set to be 1.2 T and 0.4 m, respectively. The height of the magnet gap is 10 mm. The Good Field Region (GFR)

Table 1: Design Parameters for the DC Septum Magnet

Parameters	Value
Magnetic field at pole gap	1.2 T
Effective magnet length	0.4 m
Gap height	10 mm
B · L (injected beam)	0.48 T · m
Leakage of magnetic field	$5 \times 10^5$ T
Deflecting angle	48 mrad at 3 GeV
Uniformity of magnetic field	0.1% in 4.8 mm
Distance between injected beam and stored beam	< 60 mm
Current density in coils	5 A/mm <sup>2</sup>

is defined that the field uniformity in the region is better than 0.1%. A sagitta for the injected beam trajectory in the DC septum magnet is calculated to be 2.4 mm assuming the electron energy of 3 GeV. Therefore, we set the width of GFR as twice the sagitta, e.g., 4.8 mm. The leakage field outside the septum shield should be in the same order as the geomagnetism level. Our main target in developing a DC septum magnet is that the current density in coils is less than 5 A/mm<sup>2</sup>, roughly the same as the other multipole magnets. The design parameter of the septum shield is described in Table 1.

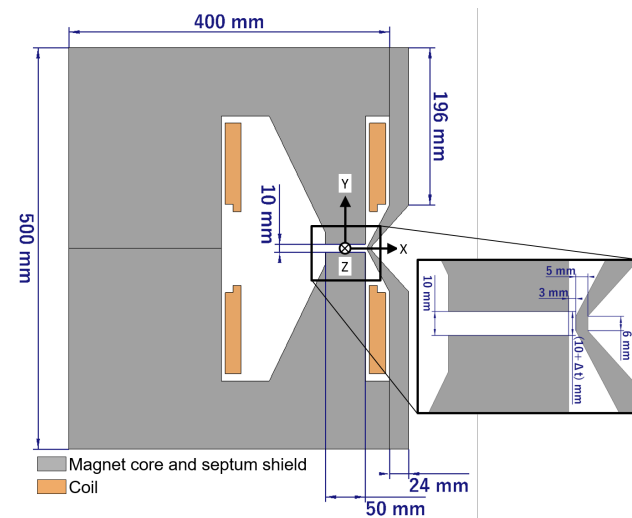


Figure 1: Schematic of the cross-section view of the DC septum magnet.

\* Work supported by RIKEN SPring-8 Center and National Institutes for Quantum Science and Technology.

<sup>†</sup> hiroshi.yamaguchi@spring8.or.jp

The magnet core and septum shield profiles are optimized using simulation code CST-STUDIO [2]. A cross-section view of the DC septum magnet is shown in Fig. 1. The septum shield has a dogleg-shaped dent at the magnet gap region [3]. This profile has three advantages points. The first advantage is that the cross-section of the coil can be enlarged, especially in the vertical direction. The coils are implemented on the side of the magnet poles. Therefore, the coil profile is free from the limitations derived from the gap height of the magnet poles and the distance of the two beams. The second advantage is that the field leakage can be suppressed. Most magnetic fluxes circulate through the magnet gap, poles, and return yoke in the magnet. Meanwhile, a part of the flux branches at the top of the magnet



Figure 2: Picture of the DC septum magnet with the magnetic shield.



Figure 3: Picture of the DC septum magnet without the magnetic shields.

and returns the gap region through the septum shield. The returned flux counteracts the absorbed flux from the magnet poles. Therefore, the leakage field outside of the septum shield is suppressed. The third advantage is that the vacuum chamber of the stored beam can be set close to the injected beam. The short distance between the injected and the stored beam reduces a betatron amplitude and contributes to stable beam operation.

The magnet core and septum shield profiles are designed to minimize the leakage field. The thickness of the shield in the gap region and the clearance between the magnet poles and septum shield are 5 mm and 3 mm, respectively. On the other hand, the thickness of the septum shield side of the magnet pole is 24 mm since it needs a sufficient volume to prevent saturation of the magnetic flux. The magnet core size is 400 mm  $\times$  500 mm  $\times$  382 mm (X  $\times$  Y  $\times$  Z). The X, Y, and Z axes are set in the horizontal, vertical, and longitudinal directions to the beam direction, respectively. In addition, two magnetic shields with 5 mm thickness are mounted to prevent field leakage in the longitudinal direction.

After the design was completed, the DC septum magnet was manufactured. Pictures of the DC septum magnet are shown in Figs. 2 and 3. The dimension errors of the magnet cores were measured using a coordinate measuring machine (CMM), and the errors were less than  $\pm 15 \mu\text{m}$ . After assembling the magnet cores, the magnet gap was also measured. The gap height of the septum shield side was 23  $\mu\text{m}$  shorter than that of the return yoke side.

## FIELD MEASUREMENTS

After the manufacture, the magnetic field in the DC septum magnet was measured. First, the injected beam trajectory was calculated in simulation using an electron with an energy of 3 GeV. Next, the integrated magnetic field,  $B \cdot L$ , on the trajectory was evaluated to sweep the coil current. Then, the coil currents at the  $B \cdot L = 0.48 \text{ T} \cdot \text{m}$  in measurement and simulation were 226 A and 231 A, respectively. In the measurement, the coil current density was  $4.5 \text{ A/mm}^2$ , and the temperature rising in the coils was  $6.2^\circ\text{C}$  with a

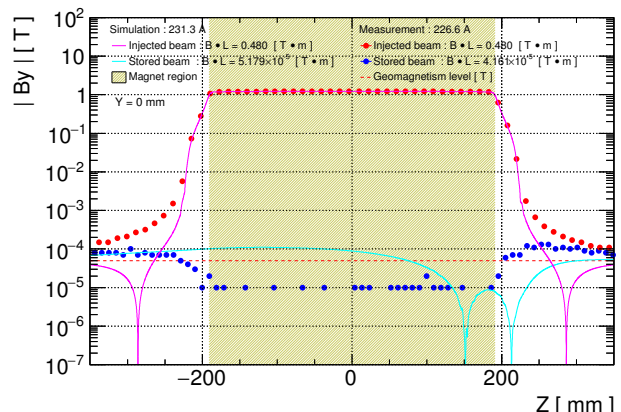


Figure 4: Magnetic field on both the injected and the stored beam trajectories.

cooling water flow of  $1.5 \text{ l/min}$ . The magnetic fields on the injected and the stored beam trajectories in measurement and simulation are shown in Fig. 4. The  $B \cdot L$ s on the stored beam trajectory in measurement and simulation were  $4.2 \times 10^{-5} \text{ T} \cdot \text{m}$  and  $5.2 \times 10^{-5} \text{ T} \cdot \text{m}$  which are comparable to the geomagnetism level of  $\sim 3 \times 10^{-5} \text{ T} \cdot \text{m}$ .

The horizontal magnetic field distribution is also shown in Fig. 5. The field strengths in measurement and simulation outside the septum shield are compatible with the geomagnetism level. Figs. 4 and 5 indicate that interference to the stored beam from this DC septum magnet is negligible while the injected beam is deflected.

Distributions of the magnetic field uniformity in the horizontal are shown in Fig. 6. Figure 6 also shows the field uniformity when the surface of the upper magnet pole is tilted. This condition is reconstructed in simulation that the gap of the return yoke side is fixed at 10 mm; meanwhile, that of the septum shield side is varied by  $(10 + \Delta t) \text{ mm}$ , and that is described in Fig. 1. The measurement distribution is consistent with that of the simulation, with a gap height of  $(10 - 0.02) \text{ mm}$  at the septum shield side. That result also agrees with the dimension measurement that the gap height

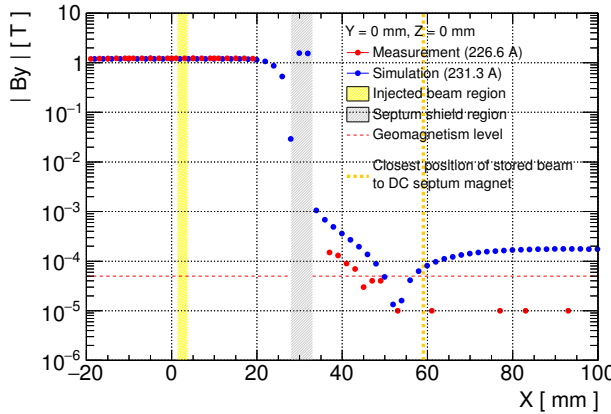


Figure 5: Magnetic field distribution in the horizontal direction at the center of DC septum magnet.

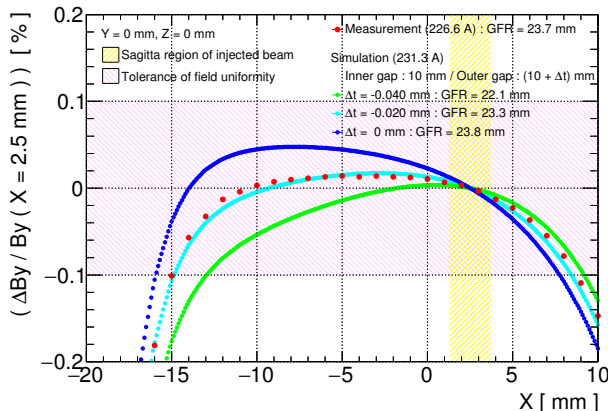


Figure 6: Uniformity of magnetic field in the DC septum magnet.



Figure 7: Picture of installation of the two DC septum magnets in NanoTerasu.

of the septum shield side was  $23 \mu\text{m}$  shorter than the return yoke side. These measurements and simulations indicate that the GFR is from  $x = -14.9 \text{ mm}$  to  $x = 8.4 \text{ mm}$ ; the width is  $23.3 \text{ mm}$ . These measurements and simulations validate that the DC septum magnet satisfies the requirement in Table 1.

## CONCLUSION

We developed the DC septum magnet with a low coil current density and electrical power consumption using the septum shield with the dogleg-shape. In our DC septum magnet, the coil current density and power consumptions are  $4.5 \text{ A/mm}^2$  and  $1 \text{ kW}$ , respectively. Meanwhile, those in the SPring-8 are  $70 \text{ A/mm}^2$  and  $40 \text{ kW}$ , respectively. Such small coil current density and power consumption lead to low-cost power supply production and accelerator operation. The magnetic field leakage is suppressed to the same order of the geomagnetism level of about  $5 \times 10^{-5} \text{ T}$ . Thus, the stored beam is not affected by the leakage field while the injected beam is deflected by the magnetic field of  $1.2 \text{ T}$ . The DC septum magnet presented in the paper and an additionally manufactured one were installed in NanoTerasu, a  $3 \text{ GeV}$  synchrotron radiation facility in Sendai, Japan [4]. The installed magnets are shown in Fig. 7. The two installed magnets were aligned with position errors of less than  $\pm 50 \mu\text{m}$ .

## ACKNOWLEDGEMENTS

The authors would like to thank SPring-8 Service Co. Ltd. and NAT Corporation for their assistance in magnetic field measurement for this work.

## REFERENCES

- [1] K. Kumagai and S. Matsui, "The injection septum magnets of the SPring-8 storage ring", *IEEE Trans. Magn.*, vol. 30, pp. 2134–2137, 1994. doi:10.1109/20.305692
- [2] Dassault Systemes, CST Studio Suite, <https://www.3ds.com/products-services/simulia/products/cst-studio-suite/>.

[3] T. Taniuchi *et al.*, “dc septum magnet based on permanent magnet for next-generation light sources”, *Phys. Rev. Acc. Beams*, vol. 23, p. 012401, 2020.  
doi:10.1103/PhysRevAccelBeams.23.012401

[4] National Institutes for Quantum and Radiological Science and Technology (QST), “Accelerator design report for 3-GeV Next-Generation Synchrotron Radiation Facility”, <https://www.qst.go.jp/uploaded/attachment/18596.pdf>